Mechanical Characteristics Analysis of Customizable Multistable Morphing Skin with Zero Poisson's Ratio

Ke Huang, Jiaying Zhang*, Qingyun Wang

School of Aeronautic Science and Engineering
Beihang University, Beijing 100190, China
*Email: jiaying.zhang@buaa.edu.cn

Abstract

This study introduces a customizable multistable morphing skin, addressing the need for stiffness anisotropy to meet the design requirements of morphing aircraft with smooth deformation and aerodynamic load-bearing. The research delves into bistable cells mechanical characteristics analysis, multistable module customization for mechanical properties, and its application in morphing wings. The approach is validated through theoretical validation, demonstrating the high customization potential of the multistable module. Proper design yields exceptional performance, reducing drive efficiency by up to 50%.

***Keywords*: camber morphing wing, multistable, morphing skin, metamaterial.**

I. INTRODUCTION

The adaptive modification of the aerodynamic profile is crucial for morphing aircraft to maintain optimal aerodynamic efficiency according to flight conditions [1,2]. However, to add degrees of freedom for deformation on the conventional fixed-geometry aircraft, further research is required in areas such as flexible substructures, distributed high-energy density actuators, flight control methods, and morphing skin [3].

Rigid aircraft skin is inadequate for flexible wings. For morphing skin, it must possess sufficient stiffness to withstand aerodynamic loads while also being flexible enough to reduce demands on actuators [4]. Addressing this conflicting design requirement, a composite morphing skin structure combining metamaterial cores and flexible surface layers has been proposed [6]. Metamaterials are artificially engineered materials with periodic structures [7]. Unlike traditional materials, metamaterials focus more on the geometric design of periodic cells to achieve desired mechanical properties by amplifying small deformations within each unit cell [7,8]. Various periodic cell shapes, such as hexagon [9], accordion [6], and corrugated panels [10], have been employed in morphing skin designs. Mechanical property studies are predominantly conducted through theoretical analysis based on Castigliano's theorem, finite element simulations, and experimental measurements, with relative stiffness as a key performance metric for evaluating mechanical metamaterial [11,12].

Despite having considerable flexibility in the deformation direction, most sandwich structures still require driving forces to maintain their deformed state. Bistable structures, possessing two stable states and enabling significant shape changes with low switching forces, can maintain configurations without driving forces [13]. Common bistable units include bistable curved beams [14], bistable shells [13], bistable hinges [15], and bistable origami mechanisms [16]. The concept of metamaterial is applied by utilizing periodic arrays, many multistable modules can be designed to achieve intricate mechanical properties. This paper introduces a multistable flexible skin based on bistable curved beam units. Theoretical analysis regarding its mechanical performance and design methodology are presented, along with a practical fabrication scheme. Finally, its application to morphing wing is demonstrated to verify its superior performance in reducing driving energy consumption.

II. THEORETICAL ANALYSIS AND CALCULATION METHOD

A. Analysis of Mechanical Properties of Bistable Units (BSU)

As shown in Figure 1, the bistable curved beam unit employed in this study is depicted. The bistable curved beam is represented by a cosine function, where a stands for twice the amplitude of the cosine function, λ represents the period length of the cosine function, t denotes the thickness of the curved beam unit, and both b and L are geometric parameters of the supporting structure.

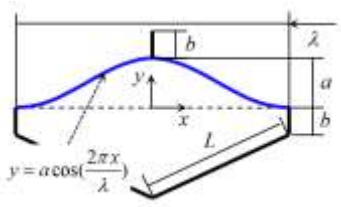

Fig. 1. Bistable curved beams unit.

Previous studies have already derived explicit expressions for the force-displacement relationship of bistable curved beams when subjected to displacement control at the midpoint.

According to the reference [14], the force-displacement response of the curved beam unit with $Q = a/t \leqslant 2.31$ can be represented as follows:

$$F_1 = \frac{3\pi^4 Q^2}{2}\Delta(\Delta - \frac{3}{2} + \sqrt{\frac{1}{4} - \frac{4}{3Q^2}})(\Delta - \frac{3}{2} - \sqrt{\frac{1}{4} - \frac{4}{3Q^2}}) \quad (1)$$

Where F_1 and Δ are normalized force and displacement, respectively, and

$$F = \frac{8 f \lambda^3}{EIh}, \Delta = \frac{d}{h} \quad (2)$$

Where E is material elastic modulus, I is moment of inertia, f is applied force, and d represents actual displacement.

As Q increases, the second or third buckling modes will be triggered. The force-displacement curve can be described by combining the curve of F_1 and curves of F_2 or F_3, where the expressions for F_2 and F_3 are

$$F_2 = 4.18\pi^4 - 2.18\pi^4\Delta \quad (3)$$

$$F_3 = 8\pi^4 - 6\pi^4\Delta \quad (4)$$

As shown in Figure 2, both F_2 and F_3 are negative-slope straight lines and are independent of the structural parameter Q. Due to the constraints of supporting structures, the appearance of the second-order mode is limited, ensuring the existence of F_3. It is related to the structural parameter Q and holds when $\Delta = 0,1,2$ is constant. When Q = 1.17, a negative stiffness segment exists along with a 'Snapthrough' phenomenon. When Q = 1.67, F_1 and F_2 are tangent to each other. When Q = 2.31, F_1 and F_3 are tangent to each other. It can be observed that a significant portion of F_3 values is less than zero, ensuring the presence of two stable states, i.e., a bistable phenomenon exists.

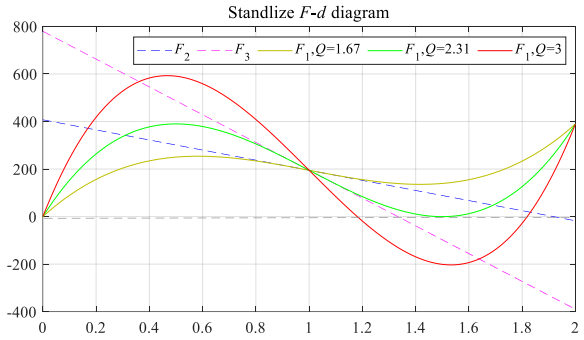

Fig. 2. Curved beam force–displacement relation.

As illustrated in Figure 3, a comparison between the force-displacement relationships of the bistable unit and the conventional honeycomb structure reveals that the switching energy between the two stable states is significantly lower than that of the traditional honeycomb structure. For the bistable curved beam, the two most important force parameters are the peak force f_{top} and the valley force f_{bot}. These parameters are represented on a cloud chart with respect to the structural parameter, as shown in Figure 4. It can be observed that the force-displacement relationship of the bistable curved beam can be designed through variations in the structural parameter. This forms a crucial foundation for the design of multistable skins.

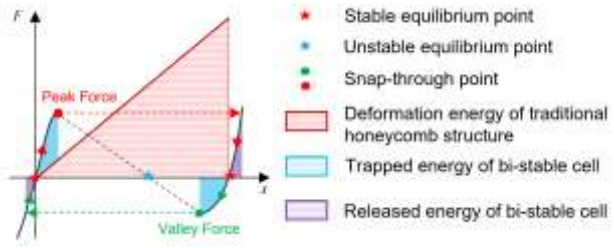

Fig. 3. Comparison between bi-stable curved cell element and traditional honeycomb structure.

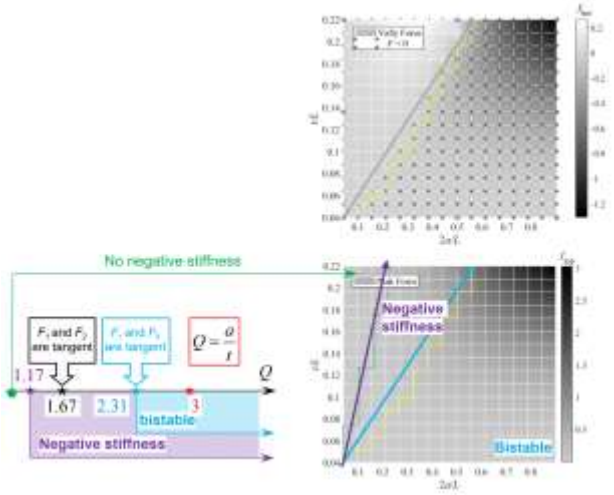

Fig. 4. The relationship between peak force and valley force and structural parameters.

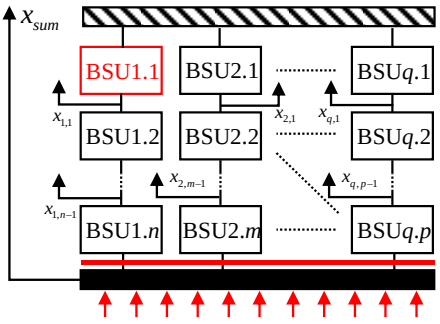

Fig. 5. Multistable modulus.

B. Analysis of Mechanical Properties of Multistable Modules (MSM)

Multistable modules can be arrayed using series and parallel combinations of bistable units, as illustrated in Figure 5. In order to simplify analytical complexity and adhere to the

design requirements of morphing skin, this study focuses on the tailored design approach of the force-displacement relationship and multistable modes using two interconnected bistable units.

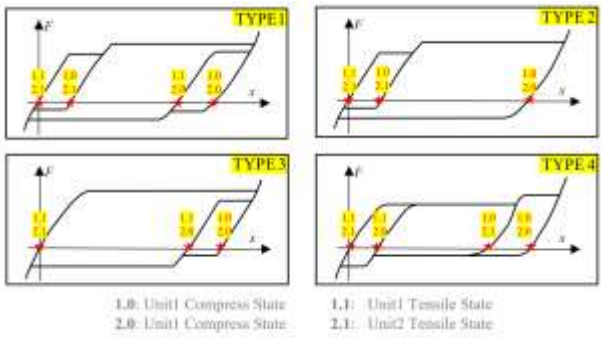

Fig. 6. Combination of two bi-stable behaviors in series.

$$d_{end_1} > d_{end_2} \begin{cases} \left|f_{top_1}\right| < \left|f_{top_2}\right| \begin{cases} \left|f_{bot_1}\right| < \left|f_{bot_2}\right| : \text{TYPE 1} \\ \left|f_{bot_2}\right| < \left|f_{bot_1}\right| : \text{TYPE 2} \end{cases} \\ \left|f_{top_2}\right| < \left|f_{top_1}\right| \begin{cases} \left|f_{bot_1}\right| < \left|f_{bot_2}\right| : \text{TYPE 3} \\ \left|f_{bot_2}\right| < \left|f_{bot_1}\right| : \text{TYPE 4} \end{cases} \end{cases} \quad (5)$$

According to reference [17], modifying the three mechanical parameters of the bistable unit allows for the realization of four distinct force-displacement curves: bistable displacement d_{end}, peak force f_{top}, and valley force f_{bot}. These four possible force-displacement curves are illustrated in Figure 6, and their corresponding relationships are described in equation (5). Since these three mechanical parameters are interconnected with the structural parameters, designing the force-displacement relationships can be achieved through the design of the bistable unit's structural parameters. Among these parameters, the crucial factors are the number and positions of the snap-through and equilibrium points.

The SQP algorithm is employed in this study to compute the force-displacement curves of the multistable modules. The bistable curved beam's two crucial structural parameters are the amplitude a and thickness t. Thus, the design of the multistable module involves modifying one parameter. Two cases are presented: 1) a = 3mm, t = 0.7/1mm; 2) a = 2/3mm, t = 0.7mm. The potential energy contour, potential energy-displacement diagram, and force-displacement relationship for these cases are depicted in Figure 7. Figure 7(a) corresponds to TYPE2 in Figure 6, exhibiting three stable equilibrium points. Similarly, Figure 7(b) corresponds to TYPE4 in Figure 6, illustrating four stable equilibrium points.

For applying the multistable module to morphing skin, two design principles can be proposed. Firstly, it is crucial to ensure the force-displacement snapthrough curve is as smooth as possible. This necessitates minimizing the size of the bistable unit concerning morphing skin and minimizing the gap between valley and peak forces among different units. In other words, ensuring a relatively even distribution of maximum and minimum values of the two critical forces. Secondly, the aim should be to maximize the number of stable equilibrium points. More equilibrium points ensure a greater number of stable states for the multistable skin. This, in turn, maintains stable configurations during loading and stretching processes, significantly aiding in reducing driving energy consumption.

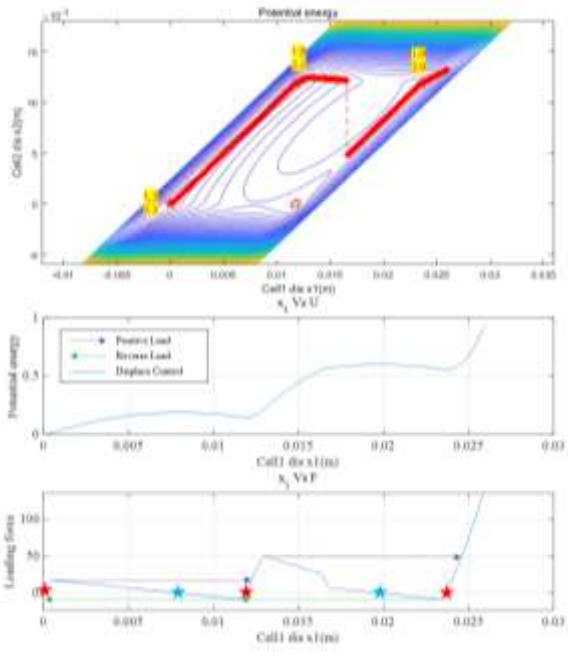

(a) a = 3mm, t = 0.7/1mm

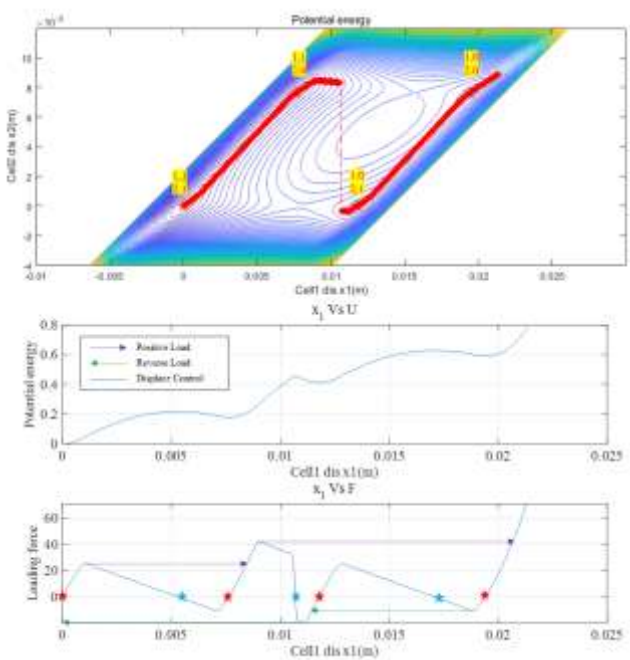

(b) a = 2/3mm, t = 0.7mm

Fig.7. Potential energy contour and load-displacement curves

III. Multi-stable Morphing skin

A. Designing Scheme

Taking the FishBAC [18], a performance-advanced camber morphing wing, as an example, a multistable skin is designed. This multistable skin comprises custom-designed multistable modules and is affixed with pre-stretched silicone skin. However, the region containing bistable curved beams is not bonded with silicone skin. In this design, multiple bistable units are placed between the longitudinal beams of the flexible section of the FishBAC. These bistable units are equally distributed between tension and compression states. During wing bending, the bistable honeycomb units in the skin under tension transition from compression to tension states, and those under compression transition conversely. During flight, the multistable honeycomb structure supports the silicone skin material, resisting out-of-plane deformations caused by aerodynamic loads to prevent flow separation. The design concept is illustrated in Figure 8.

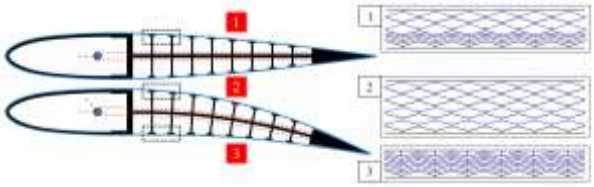

Fig. 8. Design scheme.

B. Processing and Assembly Scheme

The most crucial aspect of preparing the multistable skin lies in the fabrication of the multistable modules. Based on structural characteristics, techniques like 3D printing and laser cutting can be employed. Figure 9 illustrates the schematic of laser-cutting fabrication for the multistable modules, where different colors represent bistable units with varying mechanical properties. Furthermore, as depicted in Figure 10, the process of preparing and assembling the multistable skin involves several steps. Initially, the multistable modules undergo pre-compression. After compression, these modules are affixed onto the wing structure. Subsequently, the other side of the multistable modules is attached to the wing's longitudinal beams, completing the processing and assembly of the multistable morphing skin.

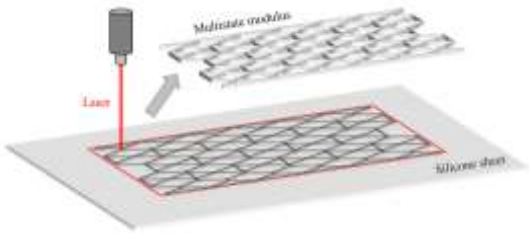

Fig. 9. Laser cutting processing.

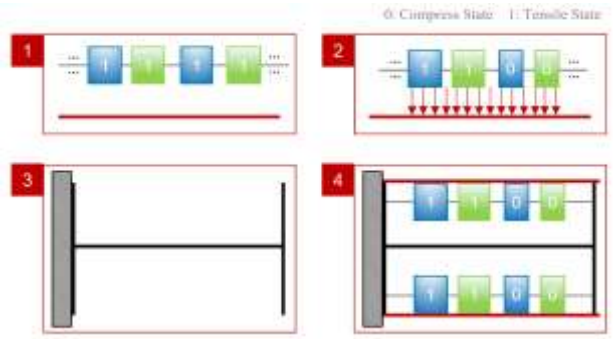

Fig. 10. Assembly process.

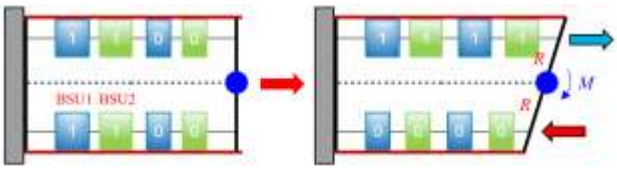

Fig. 11. Diagram of camber morphing wing.

C. Preparation and Assembly Scheme

For variable-span morphing wings, the displacement of both upper and lower skin is equivalent. However, in the case of camber morphing wings, the displacements of the upper and lower skin surfaces are equal but in opposite directions. This leads to significant differences in the force-displacement relationship. Figure 11 presents a simplified schematic, with *R*

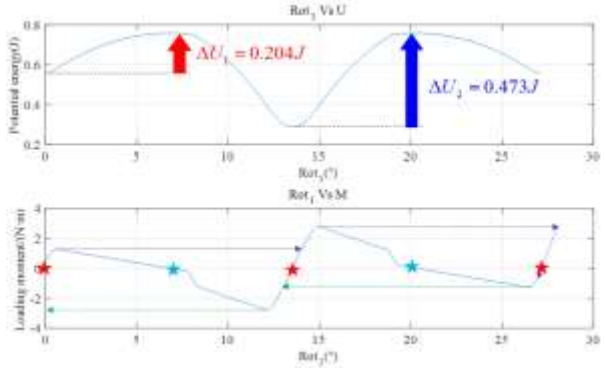

(a) a = 3mm, t = 0.7/1mm

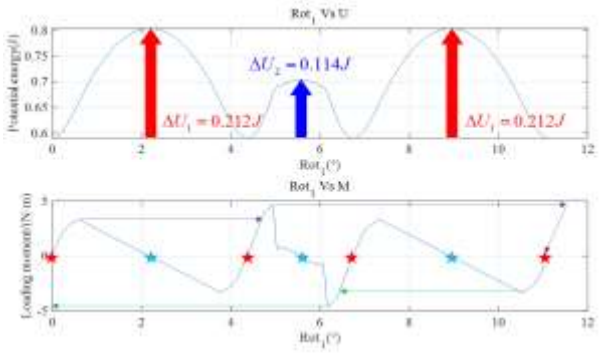

(b) a = 2/3mm, t = 0.7mm

Fig.12 The relationship between driving torque and torsion angle

= 50mm. Utilizing the multistable module analysis from Section 1.3, the relationship between the driving torque and twist angle is assessed. The overall potential energy of the structure and the torque variation with twist angle are depicted in Figure 12, with arrows indicating the energy required to overcome potential energy barriers. For both cases, the energy required for a single multistable module to overcome the potential energy barrier is 0.677J and 0.538J respectively. However, for the two constructed multistable skins, the energy required to overcome the potential energy barrier is reduced to 0.629J and 0.608J, corresponding to a reduction of 53.55% and 43.49% respectively. Therefore, the multistable modules constructed in this manner exhibit significant advantages in reducing drive energy consumption in camber morphing wings.

IV. CONCLUSION

This study introduces a multistable zero Poisson's ratio skin and investigates the mechanical characteristics of bistable analysis, customized mechanical characteristics of multistable modules, and their application in morphing wings. The following conclusions are drawn:

1. A calculation method is proposed for complex force-displacement characteristics of multistable modules composed of bistable units. Case studies are conducted to explore different advantages brought by various structural strategies, providing design insights for morphing skin.

2. Processing schemes involving laser cutting and 3D printing are proposed for the structural attributes of multistable modules. Preparation and assembly schemes for flexible wings are provided.

3. Utilizing potential energy increment analysis, the driving advantage possessed by the multistable skin is demonstrated. This validates the significant advantages of multistable skin in reducing driver requirements.

ACKNOWLEDGEMENT

This work was supported in part by the funding of the National Natural Science Foundation of China (grant number 12102017, 92271104) and the Fundamental Research Funds for the Central Universities (grant number YWF-22-L-1210).

REFERENCES

1 E. Stanewsky, "Aerodynamic benefits of adaptive wing technology," Aerospace Science and Technology, Article vol. 4, no. 7, pp. 439-452, Oct 2000.

2 S. Barbarino, O. Bilgen, R. M. Ajaj, M. I. Friswell, and D. J. Inman, "A Review of Morphing Aircraft,", Journal of Intelligent Material Systems and Structures, vol. 22, no. 9, pp. 823-877, Jun 2011.

3 G. Reich and B. Sanders, "Introduction to morphing aircraft research," Journal of Aircraft, Editorial Material vol. 44, no. 4, pp. 1059-1059, Jul-Aug 2007.

4 C. Thill, J. Etches, I. Bond, K. Potter, and P. J. T. a. j. Weaver, "Morphing skins," vol. 112, no. 1129, pp. 117-139, 2008.

5 R. M. Walser, "Electromagnetic metamaterials," in Complex Mediums II: beyond linear isotropic dielectrics, 2001, vol. 4467, pp. 1-15: SPIE.

6 E. A. Bubert, B. K. S. Woods, K. Lee, C. S. Kothera, and N. M. Wereley, "Design and Fabrication of a Passive 1D Morphing Aircraft Skin," (in English), Journal of Intelligent Material Systems and Structures, vol. 21, no. 17, pp. 1699-1717, Nov 2010.

7 S. Vasista, L. Tong, and K. C. Wong, "Realization of Morphing Wings: A Multidisciplinary Challenge," (in English), Journal of Aircraft, vol. 49, no. 1, pp. 11-28, Jan-Feb 2012.

8 J. Zheng, R. Li, W. Zhong, and Y. Li, "A bio-OCLC structure equating to a movable unit of a lattice cellular core for hybrid in-plane morphing applications," Composite Structures, vol. 235, 2020.

9 K. R. Olympio and F. Gandhi, "Flexible Skins for Morphing Aircraft Using Cellular Honeycomb Cores," Journal of Intelligent Material Systems and Structures, vol. 21, no. 17, pp. 1719-1735, 2009.

10 I. Dayyani, H. H. Khodaparast, B. K. S. Woods, and M. I. Friswell, "The design of a coated composite corrugated skin for the camber morphing airfoil," Journal of Intelligent Material Systems and Structures, vol. 26, no. 13, pp. 1592-1608, 2014.

11 Y. Chen and M. H. Fu, "Design and modeling of a combined embedded enhanced honeycomb with tunable mechanical properties," Applied Composite Materials, vol. 25, no. 5, pp. 1041-1055, 2018.

12 D. M. Boston, F. R. Phillips, T. C. Henry, and A. F. Arrieta, "Spanwise wing morphing using multistable cellular metastructures," (in English), Extreme Mechanics Letters, vol. 53, May 2022.

13 X. Tan et al., "Bioinspired Flexible and Programmable Negative Stiffness Mechanical Metamaterials," (in English), Advanced Intelligent Systems, vol. 5, no. 6, Feb 22 2023.

14 J. Qiu, J. H. Lang, and A. H. Slocum, "A curved-beam bistable mechanism," (in English), Journal of Microelectromechanical Systems, vol. 13, no. 2, pp. 137-146, Apr 2004.

15 B. Haghpanah, L. Salari‐Sharif, P. Pourrajab, J. Hopkins, and L. J. A. M. Valdevit, "Multistable shape‐reconfigurable architected materials," vol. 28, no. 36, pp. 7915-7920, 2016.

16 H. Fang, S. Li, H. Ji, and K. W. Wang, "Dynamics of a bistable Miura-origami structure," Phys Rev E, vol. 95, no. 5-1, p. 052211, May 2017.

17 Y. S. Oh and S. Kota, "Synthesis of Multistable Equilibrium Compliant Mechanisms Using Combinations of Bistable Mechanisms," (in English), Journal of Mechanical Design, vol. 131, no. 2, Feb 2009.

18 B. K. S. Woods, M. I. Friswell, "Preliminary investigation of a fishbone active camber concept," in ASME Conference on Smart Materials, Adaptive Structures and Intelligent Systems, Stone Mountain, GA, 2012, pp. 555-563, 2012.